Journal of Chromatography A, 1218 (2011) 5880–5891

Contents lists available at ScienceDirect

Journal of Chromatography A

journal homepage: www.elsevier.com/locate/chroma

Probing the interaction mode in hydrophilic interaction chromatography

Ngoc Phuoc Dinh[a,b], Tobias Jonsson[b,*], Knut Irgum[a]

[a] Department of Chemistry, Umeå University, S-901 87 Umeå, Sweden
[b] Merck SeQuant AB, Box 7956, S-90719 Umeå, Sweden

ARTICLE INFO

Article history:
Available online 17 June 2011

Keywords:
Hydrophilic-interaction chromatography
Retention factors
Selectivity
Column classification
Partial least squares

ABSTRACT

This work aims at characterizing interactions between a select set of probes and 22 hydrophilic and polar commercial stationary phases, to develop an understanding of the relationship between the chemical properties of those phases and their interplay with the eluent and solutes in hydrophilic interaction chromatography. "Hydrophilic interaction" is a somewhat inexact term, and an attempt was therefore made to characterize the interactions involved in HILIC as hydrophilic, hydrophobic, electrostatic, hydrogen bonding, dipole–dipole, π–π interaction, and shape-selectivity. Each specific interaction was quantified from the separation factors of a pair of similar substances of which one had properties promoting the interaction mode being probed while the other did not. The effects of particle size and pore size of the phases on retention and selectivity were also studied. The phases investigated covered a wide range of surface functional groups including zwitterionic (sulfobetaine and phosphocholine), neutral (amide and hydroxyl), cationic (amine), and anionic (sulfonic acid and silanol). Principal component analysis of the data showed that partitioning was a dominating mechanism for uncharged solutes in HILIC. However, correlations between functional groups and interactions were also observed, which confirms that the HILIC retention mechanism is partly contributed by adsorption mechanisms involving electrostatic interaction and multipoint hydrogen bonding. Phases with smaller pore diameters yielded longer retention of solutes, but did not significantly change the column selectivities. The particle diameter had no significant effect, neither on retention, nor on the selectivities. An increased water content in the eluent reduced the multipoint hydrogen bonding interactions, while an increased electrolyte concentration lowered the selectivities of the tested columns and made their interaction patterns more similar.

1. Introduction

Hydrophilic interaction chromatography (HILIC), which involves polar stationary phases and predominantly organic eluents, is a fast-growing sub-technique of HPLC aimed mainly at separating polar compounds that show weak retention in reversed-phase liquid chromatography [1]. The term "hydrophilic interaction chromatography" was coined by Alpert in 1990 [2], but HPLC separations based on the same principle were described fifteen years earlier for the separation of carbohydrates [3,4]. In reversed-phase chromatography, the separation of polar compounds can be assisted by techniques such as derivatization with a hydrophobic ligand [5], and by ion pairing [6]. However, these ancillary techniques make the overall process more complicated, and separation is not always achieved. Thanks to its direct approach, HILIC can provide a simpler separation without the need for derivatization reactions and modifier additions, and will also typically afford a higher sensitivity when coupled with a mass spectrometric detector [7,8]. As with most new techniques, HILIC experienced a slow start [1], but in the past few years HILIC has become a preferred technique in many life science fields involving separation of polar compounds such as pharmaceuticals [9] and toxins [10], and in emerging bioanalytical areas such as glycomics and glycoproteomics [11–14], and metabolomics [15].

Although the technique has been widely applied, the retention mechanism of HILIC is still under debate. Many studies support a postulated [2] partitioning mechanism between the bulk eluent and a water-enriched layer immobilized on HILIC phases. However, those studies also point out that the functional groups on the phase surface contribute to the selectivity in HILIC [16]. Other interactions which could be involved in HILIC are electrostatic interaction, hydrogen-bonding, dipole–dipole interaction, molecular shape selectivity, and even hydrophobic interaction [17,18]. Potentially, for solutes with more than one functionality, the retention mechanism of HILIC is multimodal, leading to "mixed mode" retention patterns which make selectivity charting a challenging task.

Mixtures of acetonitrile (ACN) with a relatively low (typically 5–40%) content of water containing a low concentration of buffering electrolyte has settled as the typical eluent composition in HILIC

* Corresponding author. Tel.: +46 90 154880; fax: +46 90 154883.
E-mail address: tobias.jonsson@merckgroup.com (T. Jonsson).

0021-9673/$ – see front matter © 2011 Published by Elsevier B.V.
doi:10.1016/j.chroma.2011.06.037

due to their good selectivity, ability to dissolve many polar solutes, and relatively low viscosity [19,20]. The separation materials used in HILIC are, on the other hand, quite diverse. As reported in a review four years ago [1], more than forty stationary phases had already been used in HILIC mode separations. The majority of those phases were silica-based, yet stationary phases based on other materials have been also reported such as zirconia [21,22], titania [23,24], and hydrophilic polymer [25,26]. HILIC phases can be uncoated (silica, zirconia, or titania) or derivatized with neutral, ionic, or zwitterionic functional groups, and systematic studies of the similarities and differences among those phases and the roles of their functional groups on the selectivity have been limited in scope. That leads to difficulties in column selection for method development using HILIC, and also a lack of guidance in development of new HILIC phases.

In reversed-phase chromatography, many methods have been developed to compare columns, and details of those tests have been extensively reviewed in the literature [27]. Most methods recently devised are based on differences in selectivities for certain solute pairs, which are selected on the basis of being representative of specific interaction modes. Chemometric techniques are then preferentially applied to classify columns. There have also been studies which attempted to make such comparisons between HILIC columns [20,28–32]. However, these comparisons only concerned specific classes of compounds such as neurotransmitters [29], peptides [30], or organic acids [31].

The aims of this work were to develop a system for comparing the selectivity of the major categories of current HILIC phases, and also to widen the understanding of interactions occurring in HILIC. As in reversed phase chromatography [27], the method chosen to elucidate selectivity and interaction modes was developed based on selectivity factors for pairs of similar chemical substances, one with properties promoting the particular interaction mode being probed, and the other member lacking such properties. Principal component analysis (PCA) was thereafter used on the obtained data to classify HILIC columns. This work also investigated the relationship between functional groups of stationary phases and the interaction mode in HILIC.

2. Experimental

2.1. Chemicals and reagents

Adenosine (≥99%), uracil (≥99%), cytosine (≥99%), 2-thiocytosine (≥99%), methylglycolate (98%), α-hydroxy-γ-butyrolactone (99%), 1-methylimidazole (99%), 1-ethylimidazole (99%), 1-vinylimidazole (99%), sorbic acid, and *cis*- and *trans*-diamminedichloroplatinum (II) were from Aldrich (Steinheim, FRG). Phenyltrimethylammonium chloride and DL-tryptophan were from Fluka (Buchs, Switzerland). Adenine, benzoic acid, benzyltrimethylammonium chloride, benzenesulfonic acid, and dihydroxyacetone were obtained from Merck (Darmstadt, FRG). Ammonium acetate was purchased from Scharlau (Barcelona, Spain). Toluene and HPLC grade ACN were from Fisher (Loughborough, UK) and deionized water (18 MΩ cm^{-1}) was supplied by a Millipore Ultra-Q (Bedford, MA) purification system.

2.2. Instrumentation

Chromatographic experiments were carried out on an HP 1050 LC system (Agilent, Palo Alto, CA) consisting of a quaternary pump, an autosampler, and a diode array detector. The ChemStation A10.01 software was used to control the HPLC system and to acquire the chromatographic data.

2.3. Selection of pairs of substances

Substances were selected in pairs that were expected to vary in their interactions in ways that might affect retention in HILIC. The test probes chosen are listed in Table 1 along with their calculated octanol–water distribution coefficients (log D) and negative logarithm of the acid dissociation constants (pK_a), and their structures are shown in Fig. 1. The potential interactions studied in this work were hydrophilic, hydrophobic, hydrogen-bonding, dipole–dipole interaction, π–π interaction, electrostatic interaction, and molecular shape selectivity.

2.4. Standards

All standard solutions of the selected test probes were prepared in the eluent at the lowest concentrations that would give a reasonable signal in UV detection. The dihydroxyacetone standards were prepared freshly every day due to their instability. The other standards were considered to be stable at room temperature except the *cis*- and *trans*-diamminedichloroplatinum (II) complexes, which were stored in a freezer at −20 °C when not in use.

2.5. Chromatographic tests

In order to make the comparison of all HILIC columns as fair as possible, the same mobile phase was used throughout; a 80:20 (v/v) mixture of ACN and 25 mM aqueous ammonium acetate, which was left in the weakly buffering neutral range with a measured pH of approximately 6.8. The eluent flow rate was fixed at 0.5 mL/min for all columns. Absorbance detection wavelengths were adjusted to obtain appropriate sensitivity and selectivity for all solutes. Retention factors were determined as the average of two injections and toluene was used as unretained marker to determine t_0. All runs were done at room temperature (22 ± 2 °C) without active thermostatting of the columns.

The chromatographic tests were performed on 22 different commercially available columns, listed in Table 2. These columns cover a wide range of properties with regards to both surface chemistry (neutral, anion exchange, cation exchange, and zwitterionic) and physical properties (particle size and pore size), and were acquired new shortly before the tests commenced. The columns were flushed with methanol, followed by 80:20 (v/v) ACN/aqueous 250 mM ammonium acetate (pH ∼ 6.8) to ensure that all counterions loaded on the columns in previous treatment steps were exchanged, and thereafter conditioned with at least thirty column volumes of eluent prior to the chromatographic evaluation.

In the study of the effect of eluent composition on selectivity, the full probe set was run on eight of the 22 columns at two additional compositions of acetonitrile and aqueous buffer, with the aqueous component consisting of either 20% (v/v) of 100 mM ammonium acetate or 30% (v/v) of 16.7 mM ammonium acetate, both at pH ∼ 6.8. Those eight columns were selected from the complete column set to include members from all the groups indicated by the PCA of the columns under the common running conditions. Effects of variations in pH and temperature were not studied in this work because changes in these variables could lead to altered properties of both the test substances and the columns; as a result, the original differences in properties between members of pairs of probe solutes might no longer pertain.

2.6. Data evaluation

Principal component analysis (PCA), a multivariable analysis technique, was used to evaluate data using the SIMCA-P+ Ver.12.0.0.0 software package from Umetrics (Umeå, Sweden). The scaling of data was set at mean-centering to shift the data towards

Table 1
Distribution coefficients and aqueous pK_a of the test solutes.

Chemical names	Abbreviations	log D[a]	pK_a[b]
Cytosine	CYT	−1.24	4.83, 9.98
Uracil	URA	−0.86	9.77, 13.79
2-Thiocytosine	S-CYT	−0.52	6.45, 9.48
Adenine	ADI	−0.55	3.15, 5.43, 9.91
Adenosine	ADO	−2.1	2.73, 5.2
N-Vinylimidazole	V-IMI	0.41	5.92[d]
N-Ethylimidazole	E-IMI	0.14	7.25[d]
N-Methylimidazole	M-IMI	−0.23	6.82
1,3-Dihydroxyacetone	DHA	−1.53	N/A
Dimethyl formamide	DMF	−0.63	N/A
Methylglycolate	M-GLY	−0.89	N/A
α-Hydroxy-γ-butyrolactone	HBL	−0.79	N/A
Phenyltrimethylammonium chloride	PTMA	−5.87	N/A
Benzyltrimethylammonium chloride	BTMA	−6.15	N/A
Benzyltriethylammonium chloride	BTEA	−5.08	N/A
Benzoic acid	BA	−1.09	4.08
Sorbic acid	SA	−0.35	5.01
Benzenesulfonic acid	BSU	−1.22	−2.36
Tryptophan	TRP	−3.7	2.54, 9.4, 16.6
cis-Diamminedichloroplatinum (II)	CDDP	−2.19[c]	N/A
trans-Diamminedichloroplatinum (II)	TDDP	–	N/A
Toluene	TOLU	2.49	N/A

N/A, not applicable. When not otherwise noted, the log D, and pK_a values were calculated by Marvin Calculator Plugins from ChemAxon [50].
[a] log D, logarithm of octanol–water partition coefficient at pH 6.8 including ionic species.
[b] pK_a, negative logarithm of acid dissociation constants determined in water.
[c] The value is from Ref. [49].
[d] Values from Ref. [34].

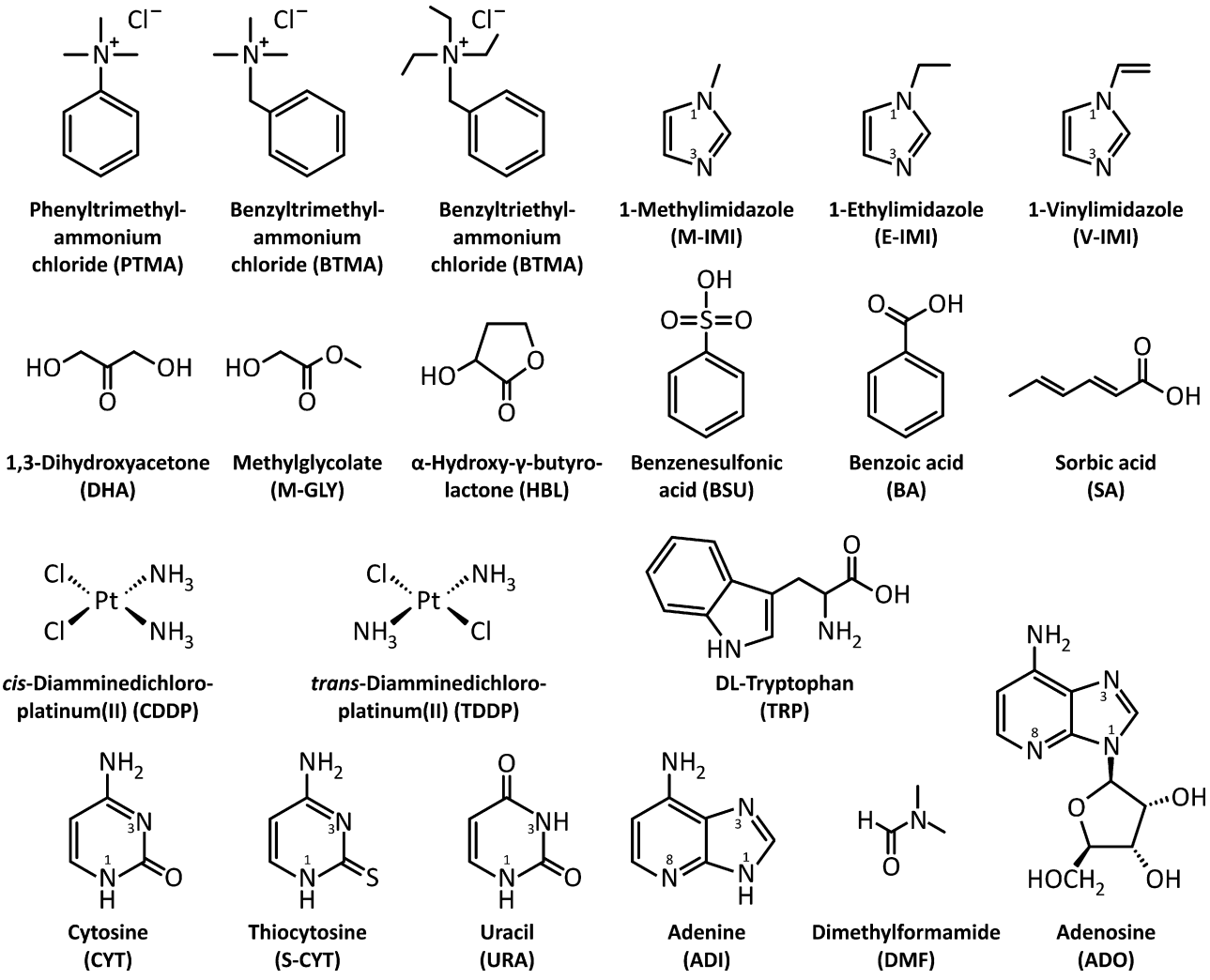

Fig. 1. Structures of test solutes used in this work.

Table 2
Parameters of tested columns.

No	Brand name	Manufacturer	Support	Functionality	Particle size (μm)	Pore size (Å)	Surface area (m^2/g)	Column size[a] (mm)
1	ZIC-HILIC	Merck	Silica	Polymeric sulfoalkylbetaine zwitterionic	5	200	135	4.6 × 100
2	ZIC-HILIC	Merck	Silica	Polymeric sulfoalkylbetaine zwitterionic	3.5	200	135	4.6 × 150
3	ZIC-HILIC	Merck	Silica	Polymeric sulfoalkylbetaine zwitterionic	3.5	100	180	4.6 × 150
4	ZIC-pHILIC	Merck	Porous polymer	Polymeric sulfoalkylbetaine zwitterionic	5	–	–	4.6 × 50
5	Nucleodur HILIC	Macherey-Nagel	Silica	Sulfoalkylbetaine zwitterionic	5	110	340	4.6 × 100
6	PC HILIC	Shiseido	Silica	Phosphorylcholine zwitterionic	5	100	450	4.6 × 100
7	TSKgel Amide 80	Tosoh Bioscience	Silica	Amide (polymeric carbamoyl)	5	80	450	4.6 × 100
8	TSKgel Amide 80	Tosoh Bioscience	Silica	Amide (polymeric carbamoyl)	3	80	450	4.6 × 50
9	PolyHydroxyethyl A	PolyLC	Silica	Poly(2-hydroxyethyl aspartamide)	5	200	188	4.6 × 100
10	LiChrospher 100 Diol	Merck	Silica	2,3-Dihydroxypropyl	5	100	350	4.0 × 125
11	Luna HILIC	Phenomenex	Silica	Cross-linked diol	5	200	185	4.6 × 100
12	PolySulfoethyl A	PolyLC	Silica	Poly(2-sulfoethyl aspartamide)	5	200	188	4.6 × 100
13	Chromolith Si	Merck	Silica monolith	Underivatized	N/A	130	300	4.6 × 100
14	Atlantis HILIC Si	Waters	Silica	Underivatized	5	100	330	4.6 × 100
15	Purospher STAR Si	Merck	Silica	Underivatized	5	120	330	4.0 × 125
16	LiChrospher Si 100	Merck	Silica	Underivatized	5	100	400	4.0 × 125
17	LiChrospher Si 60	Merck	Silica	Underivatized	5	60	700	4.0 × 125
18	Cogent Type C Silica	Microsolv	Silica	Silica hydride ("Type C" silica)	4	100	350	4.6 × 100
19	LiChrospher 100 NH_2	Merck	Silica	3-Aminopropyl	5	100	350	4.0 × 125
20	Purospher STAR NH_2	Merck	Silica	3-Aminopropyl	5	120	330	4.0 × 125
21	TSKgel NH_2-100	Tosoh Bioscience	Silica	Aminoalkyl	3	100	450	4.6 × 50
22	LiChrospher 100 CN	Merck	Silica	3-Cyanopropyl	5	100	350	4.0 × 125

N/A, not applicable. All data on particle size, pore size, and surface area are taken from catalogues and websites of manufacturers.
[a] Column dimensions are given as inner diameter by length.

the mean, and unit-variance to equalize the variances of variables. Thereby, the mean of distribution of observation would shift to the center of axis system and the data would be more objective. Because of the mean-centering and scaling, axis scales are omitted in Figs. 3–9; the shaded circles represent unit variance.

3. Results and discussion

3.1. HILIC columns

Based on information on the type of surface functional groups, the 22 columns selected for this test were preliminarily classified into four groups; zwitterionic (columns 1–6), neutral (columns 7–11 and 22), cation exchange (columns 12–18), and anion exchange (columns 19–21). Since the pH of all the eluents used was close to neutral (pH of the aqueous part prior to mixing was ~6.8), silanol groups on the underivatized silica columns were expected to be deprotonated, yielding negatively charged surface groups that are capable of acting as cation exchange sites. Conversely, the amino columns would have their functional groups protonated as positively charged, and would therefore have anion exchange properties. Some columns possessed similar functional groups but differed in particle size, pore size, bed morphology (particulate/monolithic), or manufacturer. The LiChrospher CN cyanopropyl column was initially included as well. However, on this column some of the hydrophilic test solutes (notably uracil, cytosine, and dihydroxyacetone) were eluted *faster* than the toluene used as hydrophobic void volume marker. This verified the low potential of cyanopropyl silica as a material for HILIC, and the LiChrospher CN column was therefore excluded from further study.

3.2. Substance pairs selected as probes for investigation of interaction modes

The choice of substances for investigating the interaction modes was based on principles similar to those used for selection of test solutes in reversed phase [27], with appropriate modifications made for the kind of interactions expected to be pertinent to HILIC. A primary selection criterion was a low (preferably negative) logarithm of the octanol–water partitioning coefficient (see below). Although it is virtually impossible to find solute pairs which differ only in a single interaction mode and otherwise behave identically, we have tried to find a range of substance pairs that are as close to the ideal as possible, which are also commercially available in sufficient purity at reasonable cost. The substance pairs and primary interactions intended to be probed by each pair are listed in Table 3.

Hydrophilic interaction is generally accepted as being implemented by the distribution of solutes between the bulk eluent and the water-enriched layer on the surface of the stationary phase [1,2], and the retention in HILIC has recently been shown to correlate well with the octanol–water partition coefficient of the compounds being separated [33]. Hydrophobic interaction is normally assessed by the selectivity for two solutes which differ by one $-CH_2-$ group, denoted as α_{CH_2}. Ethylbenzene and toluene, or pentylbenzene and butylbenzene have often been used as pairs in reversed-phase HPLC to determine α_{CH_2}. In this work, 1-ethylimidazole and 1-methylimidazole were chosen to serve as the α_{CH_2} probe pair, since the diazole ring is polar enough to afford acceptable retention in HILIC. Alkylation has little influence on the pK_a of the ^{1}N (pyridine-like) amine functionality in imidazoles (the pK_a of imidazole is 7.12 and that of 1-ethylimidazole 7.25) [34]. These diazole solutes are therefore expected to be slightly protonated (to a similar degree) and hence possess some posi-

tive charge under the test conditions in this work. The retention of imidazoles in HILIC should mainly be attributable to resonance-mediated charge separation in the diazole ring, and the hydrogen bond acceptor properties of the ^{3}N imine nitrogen. The hydrogen bond donor properties prominent in unsubstituted imidazole are expected to be disrupted by the alkyl substitution of the selected probes [35].

The degree of hydrogen bonding was probed by three solute pairs; dimethylformamide/dihydroxyacetone, adenosine/adenine, and dihydroxyacetone/methylglycolate, which all differ in the number and type of potential hydrogen bonds. Adenosine and adenine differ by one ribose residue which thus was assumed to significantly increase the hydrogen bonding interaction. Phenyltrimethyl, benzyltrimethyl, and benzyltriethyl ammonium ions were used to probe cation exchange interaction. The advantage of using quaternary ammonium ions instead of the amines often used in reversed-phase is that their charge is independent of pH. Benzenesulfonic acid, benzoic acid, and sorbic acid are negatively charged at pH 6.8 and therefore suitable for determination of anion exchange interactions. In the study of electrostatic interaction (cation exchange, anion exchange), cytosine was used as reference in all pairs to compensate for the hydrophilic interaction. Cytosine was chosen for this task because it is neutral at the testing conditions, and in comparison with other neutral substances selected it has the highest hydrophilicity and a greater structural similarity to the substances that were selected for probing electrostatic interaction. Tryptophan (TRP) has a p*I* of 5.89 in water [36] and exists almost solely in the zwitterionic form in water at neutral pH [37]. Since the ratio of zwitterionic to undissociated form is a function of the dielectric constant of the medium [38], it will be lower at elevated ACN concentrations. Its prototropic ratio is also most likely affected by the chemical microenvironment in the stationary phase interaction layer [39]. Still TRP constitutes a reasonable choice for probing selectivity for zwitterions, paired with adenine, due to their similar structures. Vinyl- and ethylimidazole differ only by the double bond in the substituent and were chosen to probe π–π interaction.

The solutes chosen to probe dipole–dipole interaction were *cis*- and *trans*-diamminedichloroplatinum (II), which are both planar, uncharged complexes. Because of the asymmetric orientation of the ammine- and chloro-ligands, *cis*-diamminedichloroplatinum (II) has a dipole moment, which is lacking in the *trans* isomer because of the symmetric ligand pattern. The difference in retention of *cis*- and *trans*-diamminedichloroplatinum (II) should therefore be representative of dipole–dipole interaction. This solute pair could possibly also be a probe set for differences in steric accessibility of the preferred binding site to the stationary phase. Molecular shape selectivity was determined by two pairs; sorbic acid and benzoic acid (differing in the size and shape of the hydrophobic part of the molecule), and methylglycolate and α-hydroxy-γ-butyrolactone (which differ in the orientation and flexibility of the hydrophilic part).

It should be realized that all chosen pairs are likely to probe other interactions to some extent, in addition to those primarily intended. It has for instance recently been shown that substances can be oriented while approaching HILIC phases during the elution [42], which could affect the intended probing interactions.

3.3. Retention on HILIC columns

Retention was first evaluated by the average retention factor of neutral test substances on all twenty-one columns left after the cyanopropyl column had been excluded (Fig. 2). Among the columns tested, LiChrospher Si 60 showed the overall strongest retention, while Chromolith Silica and Luna HILIC showed the lowest overall retention for neutral compounds. Among the remaining columns, ZIC-HILIC (3 μm, 100 Å), TSK-Amide 80 (3 μm), and PolySulfoethyl A provided the longest retention for neutral solutes. As opposed to the results reported by Alpert [2], PolySulfoethyl A showed 30% *higher* retention in our experiments than did PolyHydroxyethyl A.

Although this work focused on classification of columns in terms of retention and selectivity, and thus did not consider peak shape as evaluation criterion, some columns showed peak tailing or fronting for some substances under the test conditions used in this work. Notably, the cation exchange probes PTMA, BTMA and BTEA exhibited a tailing on several of the tested columns so severe that it would be hard to use them for the purpose of separating these substances (data not shown).

Retention on HILIC columns was also evaluated by PCA of the retention data set of the test substances. Initial fittings (Fig. 3a) showed that the LiChrosphere Si 60 column caused a strong bias due to its high retention relative to the other columns. It was therefore excluded in this analysis to allow a clearer modeling. The score-loading biplot of the remaining columns and all substances (Fig. 3b) shows that the columns could be classified into three distinct groups according to their surface chemistry: (a) unfunctionalized silica, with Chromolith Si and the Cogent Type C positioned in each end of a rather drawn-out banana-shaped cluster; (b) columns with amino functionality; and (c) the remaining columns including neutral, zwitterionic, and PolySulfoethyl A. As can be seen in Fig. 3b this grouping was to a large extent based on the retention of the cationic and anionic test substances, and confirms that electrostatic interaction plays an important role for the retention of charged solutes in HILIC, on columns with distinct anion or cation exchange functionality.

3.4. Correlation between retention of substances and log D

In an "inverted" scrutiny of the data, the PCA was done with the dataset involving the columns as variables and the retention factors of the substances as observations. Although the functionalities of the columns are diverse, it should be noted that the distribution of

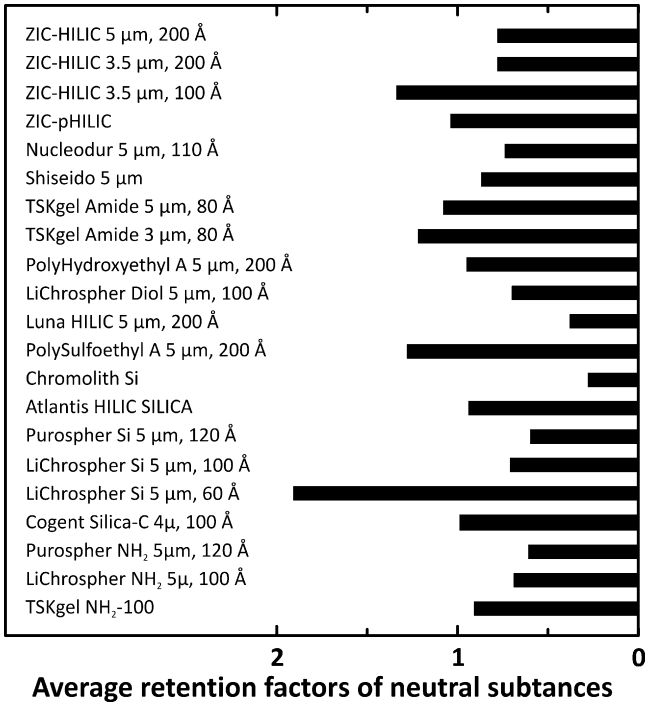

Fig. 2. Average retention of neutral solutes on HILIC columns.

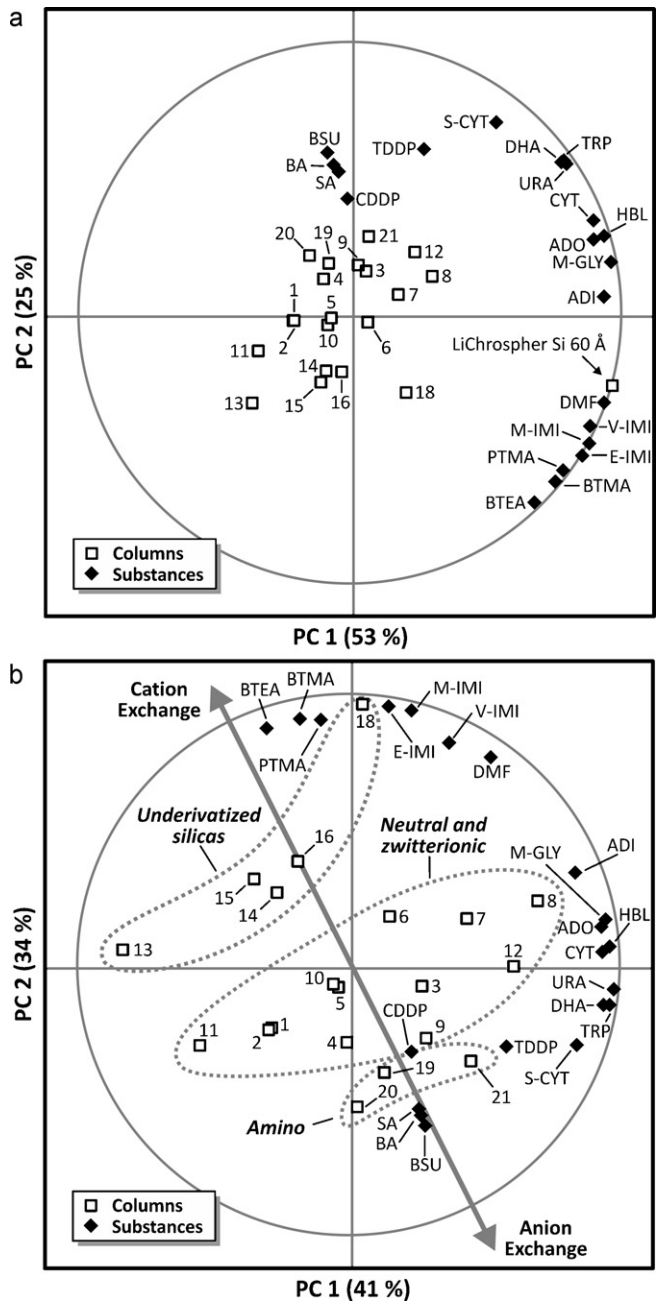

Fig. 3. Score and loading biplot of the two first components of the model where the variables were the retention factors of the selected probe substances, and the observations were (a) the entire column set or (b) all columns except the LiChrospher Silica 60 Å (column 17). For column numbering, see Table 2.

substances in each of the groups identified was surprisingly linear, as hinted by the dotted lines in Fig. 4a. A hidden parameter may still exist that influenced the distribution of substances. As mentioned in the introduction, partitioning is now generally believed to be the primary retention mechanism in HILIC. It is therefore not unlikely that a latent variable related to partitioning had impact on the distribution of columns in each of the groups identified in the model in Fig. 4a. Therefore, an additional PCA was carried out on a modified data set, where log *D*, the logarithm of the octanol–water distribution coefficient at pH 6.8, was added as a variable. Test solutes CDDP and TDDP were excluded due to unavailability of their log *D* values. The score and loading biplot of the two first components (Fig. 4b) showed that the log *D* variable was located in the lower left quadrant, almost on an extension of the distribution of the neutral substances, *i.e.*, on the distribution line for HILIC interactions not affected by electrostatic interaction. It should also be noted that the inclusion of log *D* in the model caused practically all columns to move further away towards the upper right quadrant, yet their relative positions was largely maintained. A tempting and also rational interpretation is that positive log *D* values, which in a general sense means higher hydrophobicity, counteracts HILIC interactions. The retention times would then be based mainly on the differences in log *D* values of the substances, and constitute a direct evidence that partitioning is the main retention mechanism in HILIC.

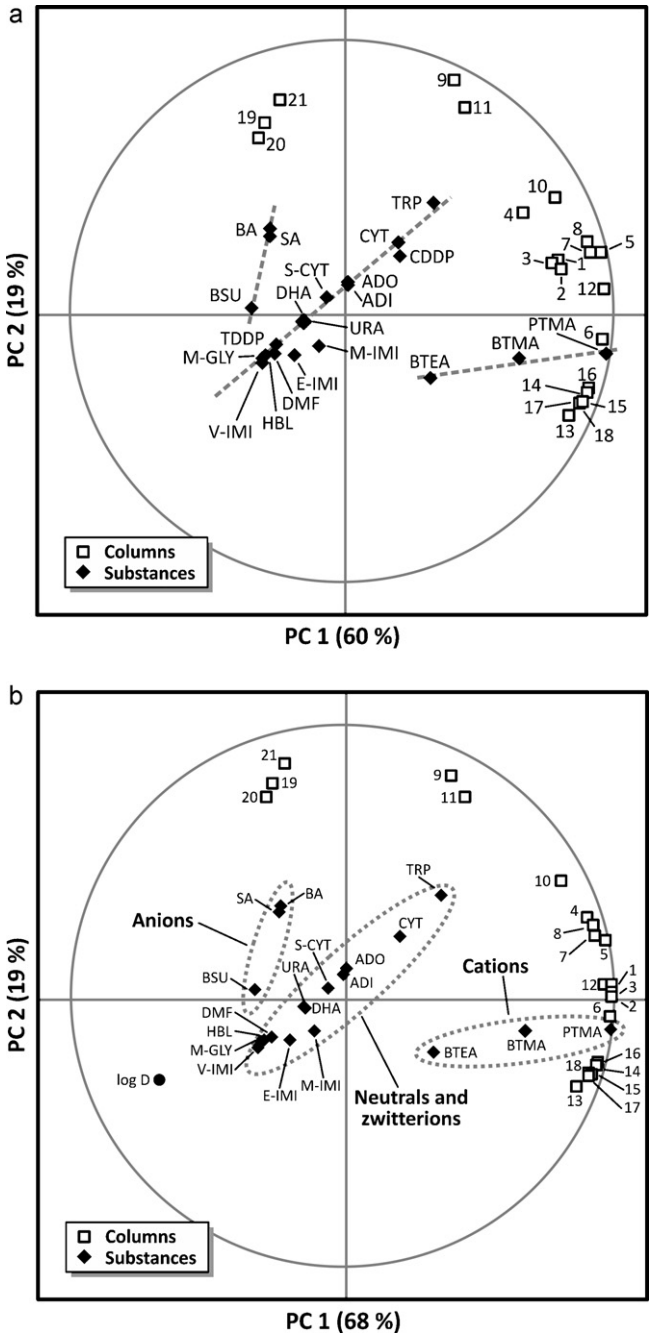

Fig. 4. Score and loading biplot of the two first components of the model where the variables were (a) all retention factors on all columns or (b) the retention factors of selected substances on the columns and log *D* of those substances, and the observations were (a) all test solutes or (b) all test solutes with the exception of CDDP and TDDP. For column numbering, see Table 2.

Table 3
Test solutes selected for selective probing of interactions in HILIC sorbents.

Targeted primary interaction	Probing pairs[a]	log *D* ratio[b]
"Hydrophilic"	CYT/URA	1.4
"Hydrophilic"	CYT/S-CYT	2.4
Hydrophobic	E-IMI/M-IMI	−0.6
Hydrogen bond donor	DHA/M-GLY	1.7
Multipoint hydrogen bonding	DHA/DMF	2.4
Multipoint hydrogen bonding	ADO/ADI	3.8
Hydrophilic shape selectivity (oriented hydrogen bonding)	M-GLY/HBL	1.1
Dipole–dipole interaction	CDDP/TDDP	N/A
π–π interaction	V-IMI/E-IMI	2.9
Cation exchange	PTMA/CYT	4.7
Cation exchange	BTMA/CYT	5.0
Cation exchange	BTEA/CYT	4.1
Anion exchange	BSU/CYT	1.0
Anion exchange	BA/CYT	0.9
Anion exchange	SA/CYT	0.3
Zwitterionic (quadrupolar electrostatic)	TRP/ADI	6.7
Hydrophobic shape selectivity	SA/BA	0.3

[a] For designations, log *D* values, and structures, see Table 1 and Fig. 1.
[b] Calculated from the log *D* values given in Table 1.

3.5. Selectivity on HILIC columns

A PCA was thereafter made on the data set constructed from the separation factors of the pairs of substances selected to probe for selectivity (Table 3) as variables and the columns as observations. There were a total of 15 variables and 21 observations. With the two first principal components, the model covered more than 70% of the total variance and the validity was also high with a Q2 cross-validation value of 0.486. The score-loading biplot (Fig. 5) shows that the columns were now clustered in four main groups: (1) the neutral columns; (2) the amino columns; (3) the silica columns including Chromolith; and (4) ZIC-HILIC, ZIC-pHILIC, and PolySulfoethyl A. Groups 2, 3, and 4 formed a triangle with the "neutral" columns (Group 1) in the center. The Nucleodur HILIC and Shiseido PC HILIC columns were situated close to the center of the plot and

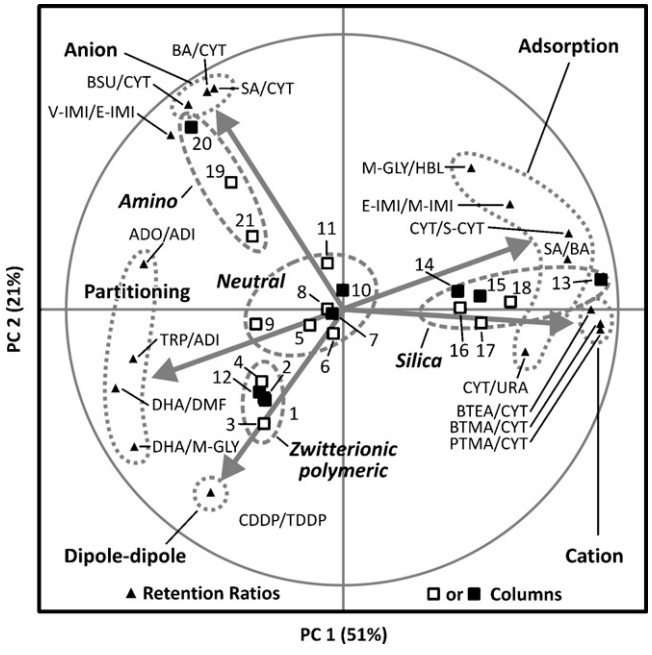

Fig. 5. Score and loading biplot of the two first component of the model where the observations were the columns and the variables were the retention ratios of all test substance pairs. For column numbering, see Table 2.

thus grouped with the neutral columns, but slightly offset in the same direction as the other zwitterionic columns (Group 4). Both the Nucleodur HILIC and Shiseido PC HILIC columns are described by the manufacturers as being zwitterionic, but in this study they turned out to be more similar to the neutral columns than to the ZIC-HILIC and ZIC-pHILIC columns, which made up the larger part of a tight cluster that was oriented towards the dipole–dipole probe pair CDDP/TDDP. To our knowledge, both the Shiseido PC HILIC [40] and Nucleodur HILIC [41] columns are made by the conversion of silanol groups into ligands with single phosphorylcholine and sulfobetaine moieties, respectively, through conventional silane chemistry, whereas the interactive layers of the ZIC-HILIC and ZIC-pHILIC columns are made up by a polymer layer carrying one sulfobetaine moiety for each monomeric unit. In contact with water, such polyelectrolyte layers are prone to form hydrogels. This is a substantial difference in attachment chemistry, which may explain the different selectivity patterns of the monomerically functionalized zwitterionic columns compared to the ZIC-HILIC and ZIC-pHILIC columns. This also suggests that zwitterionic columns with low ligand loading behave as if they are essentially neutral, which is also reasonable since zwitterions are balanced in charge.

The grouping of PolySulfoethyl A within the rather tight cluster formed by all the ZIC-HILIC and ZIC-pHILIC columns was rather surprising. The intended sulfoethyl functionality of PolySulfoethyl A should make it a strong cation exchanger, and we therefore expected to see a retention pattern more similar the unmodified silica columns, which are assumed to express substantial cation-exchange properties at the eluent pH used. The similarity of the PolySulfoethyl A selectivity pattern with those of the polymeric sulfobetaine zwitterionic columns could perhaps be accounted for by reviewing the synthesis procedure of PolySulfoethyl A, which involves as the first step a modification of aminopropyl silica particles with poly(succinimide), followed by reaction with taurine [43]. It is quite unlikely that *all* the amine groups of the aminopropyl silica starting material are occupied by binding to the polymeric coating after the first reaction step. If such residual amine groups exist, they would be positively charged under the test conditions and could, together with the sulfonate groups, form a polymeric phase that possesses zwitterion-like properties. The relative position for the PolyHydroxyethyl A column (which is synthesized using a similar procedure [2]) situated between the zwitterionic column group and the amino column cluster do support this rationale. However, weak but distinct cation exchange properties caused by sufficient ion exchange capacity in the ZIC-HILIC and ZIC-pHILIC columns could also contribute to the grouping of these columns together with the PolySulfoethyl A column. The unexpected grouping of the PolySulfoethyl A column highlights that not only distal and intended functional groups contribute to the retention of solutes in HILIC, but possibly also functional groups buried deeper inside, or underneath, the coating layer.

By looking at the loading of the two first components of the model, we could gain more knowledge on the factors that differentiate HILIC columns. The first principal component, which accounted for more than 50% of the variance in the data, had significant contributions from all solute pairs except SA/CYT and CDDP/TDDP. The second principal component which covered 21% of the variance in the data was mainly contributed by CDDP/TDDP and V-IMI/E-IMI, and by the anion exchange probe pairs. The pairs intended to probe for cation exchange properties had the largest positive contribution to the first component, while the pairs chosen to probe for anion exchange properties had the largest positive contribution to the second principal component. The narrow clusters reveal that pairs designed to probe cation exchange properties were well correlated, as were the probe pairs for anion exchange. The locations of both these tight clusters close to the perimeter of the plot indicates that ion exchange was a dominant component in

the HILIC retention model for charged solutes separated on columns with unipolar charge. It also tells us that ion exchange *per se* offers limited selectivity apart from electrostatic interaction based on net charge, which was also noted by Alpert and Andrews [43]. A parallel can be drawn to 2D-HPLC separation of peptides using strong cation exchange in the first dimension, where peptides with different net charges tend to cluster in rather narrow elution windows because selectivity in ion exchange is driven mainly by solute charge [44].

The next observations worth pointing out are that the tight clusters containing the anion exchange and cation exchange solute pairs were not situated diametrically opposite each other on the loading plot, and that the anion and cation exchange propensities were resolved as positive contributors to *separate* principal components. That tells us that *at least* one additional strong interaction mode contributed to the selectivity among the columns, and the probe pairs responsible for this would be found in the left/lower left or right/upper right parts of the loading plot in Fig. 5. As a matter of fact, in these two regions, two diverse, yet distinct clusters of solute pairs could be identified. To the right, with high positive scores in the first principal component, probe pairs for shape selectivity, "hydrophilic", and hydrophobic interactions were clustered in a rather wide region overlapping the cation exchange probes. Common to the probe pairs in this cluster were the relatively similar solute structures and close relative position of the individual probes along the distribution line for neutral solutes coordinating with the log *D* value (*cf.* Fig. 4b). Most of the probe pairs in this cluster also had small log *D* ratios (*cf.* Table 3), ranging from −0.6 for E-IMI/M-IMI to 2.4 for CYT/S-CYT, highlighting their similarity in structure and thus also in relative hydrophilicity. The positioning of the pair probing hydrophilic shape selectivity (M-GLY/HBL), together with other pairs with limited flexibility in their hydrogen bond donor and acceptor groups (e.g., CYT/URA), in this group also indicates that the hydrogen bonding is more *oriented*, and that interaction of the probes with the stationary phase take place on only a few positions, *i.e.*, quite similar to an adsorption mechanism. The fact that this group of structurally similar pairs pulled the model in the same direction as the cation exchange probes should not be interpreted as a connection between cation exchange and these interactions, but rather indicate a correlation between both these probe pair categories and the underivatized silicas, among those columns included in this study. Situated to the left, almost opposite to the above group, was a similarly diverse cluster of probe pairs with high negative scores in the first principal component. This left cluster contained solute pairs aimed to probe zwitterionic interactions, multipoint interaction, and hydrogen bond donor interactions. Common to the probe pairs in this cluster were a relatively larger structural diversity and corresponding larger log *D* value ratios (between 1.7 and 6.7; *cf.* Table 3). All probe pairs in this cluster were molecules with *multiple* and *flexible* positions for their hydrogen bond donor and acceptor groups, indicating that several interaction points can, and probably are, responsible for the selectivity. In summary, we interpret these two clusters of probe pairs as assessing selectivity dominated by partitioning (left cluster) *vs.* selectivity dominated by oriented hydrogen bonding and ultimately adsorption (right group).

The two pairs CYT/URA and CYT/S-CYT aimed at probing hydrophilicity were not correlated as strongly as expected. At the near neutral eluent pH chosen for these tests, S-CYT should be substantially protonized (its aqueous pK_{a1} is 6.45), whereas CYT (pK_{a1} 4.83) should be very little protonated. CYT/S-CYT might therefore also inversely probe cation exchange interactions, so CYT/URA appears to be the more proper pair to use as probes for hydrophilic interaction under these test conditions. The V-IMI/E-IMI pair turned out to be strongly correlated with the anion exchange probe pairs rather than with π–π interaction, which was the intended probe function. On reviewing their pK_a values [34], this was found to be rational, since the pK_a of V-IMI is 5.92 and that of E-IMI is 7.25. Under the eluent conditions used in the present study, the degree of positively charge of E-IMI should therefore be substantially higher than that of V-IMI, and the V-IMI/E-IMI pair would thereby act inversely as a probe for cation exchange interactions. Since electrostatic interactions seemed to overshadow other interaction modes for charged solute pairs, the V-IMI/E-IMI pair must be considered as unfit for the purpose of probing for π–π interactions, at least on columns expressing pronounced ion exchange properties and at pH values where they differ in charge. No conclusions can thus be drawn on this interaction type from the full model based on probe pairs in Fig. 5, since V-IMI/E-IMI was the only probe pair selected with this intended function.

By matching the loading to the score (Fig. 5), one can thus discern two main trends in the distribution of columns on the score plot. The first trend was electrostatic interaction, with (i) the silica columns separated from the other columns due to the cation exchange properties of dissociated silanols and (ii) the amino columns exhibiting anion exchange properties. The other prevailing selectivity trend seemed to be hydrophilic partitioning by multipoint interaction and dipole–dipole interaction *vs.* adsorption-like selectivity by oriented hydrogen bonding and single point interaction. It was furthermore possible to discriminate between the zwitterionic columns and the others due to those interactions, where the zwitterionic columns (including PolySulfoethyl A) were distributed in the direction of the solute pair intended to probe for dipole–dipole interactions. Compared to the score plot of the model based on raw retention factors only (Fig. 3b), the model based on retention ratios of selective solute pairs in Fig. 5 provided a different and considerably clearer characterization of the HILIC columns. The substantial difference between these two models also implies that retention and selectivity were not related in a way that could be immediately uncovered by comparing the models. This is, on the other hand, quite reasonable since retention and selectivity are not necessarily strongly correlated.

3.6. Discrimination in electrostatic interactions

Since the interaction mode of the amino and unmodified silica columns appeared to be dominated by electrostatic interactions, we decided to carry out a couple of principal component analyses on different sub-sets of the data, and in the first one of these we excluded all probe pairs designated for testing anion and cation exchange interactions. This should to a large extent remove contributions to selectivity from strong electrostatic interactions (ion exchange), and we expected to see a clearer correlation between the columns and the remaining polar interaction modes. The model produced by this reduced data set is shown in Fig. 6a. Observations that can be made in this model is that the silica columns are still clustered as tightly as before, with high positive contributions to the first principal component, and that the positive correlation with the single point interaction probes and a negative correlation with multipoint probes remained essentially unchanged. This persistent juxtaposition of the single- and multipoint interaction probe pairs strengthens our conclusions of (a) a larger contribution of adsorptive interactions on the unmodified silica columns and (b) better opportunities for multipoint interactions on materials with highly hydrophilic polymeric interactive layers that likely are prone to swell into hydrogels in partly aqueous eluents. When the structures of the probes are studied, it also becomes apparent that a common feature of several of the probe pairs associated with the silica columns is their pronounced possibilities for *oriented* hydrogen bonding. This applies in particular to the M-GLY/HBL pair, where the ring will lock the orientation of both the hydrogen bond donating and the two hydrogen bond accepting groups. Strong orientation of the hydrogen bonding donor and acceptor capabilities

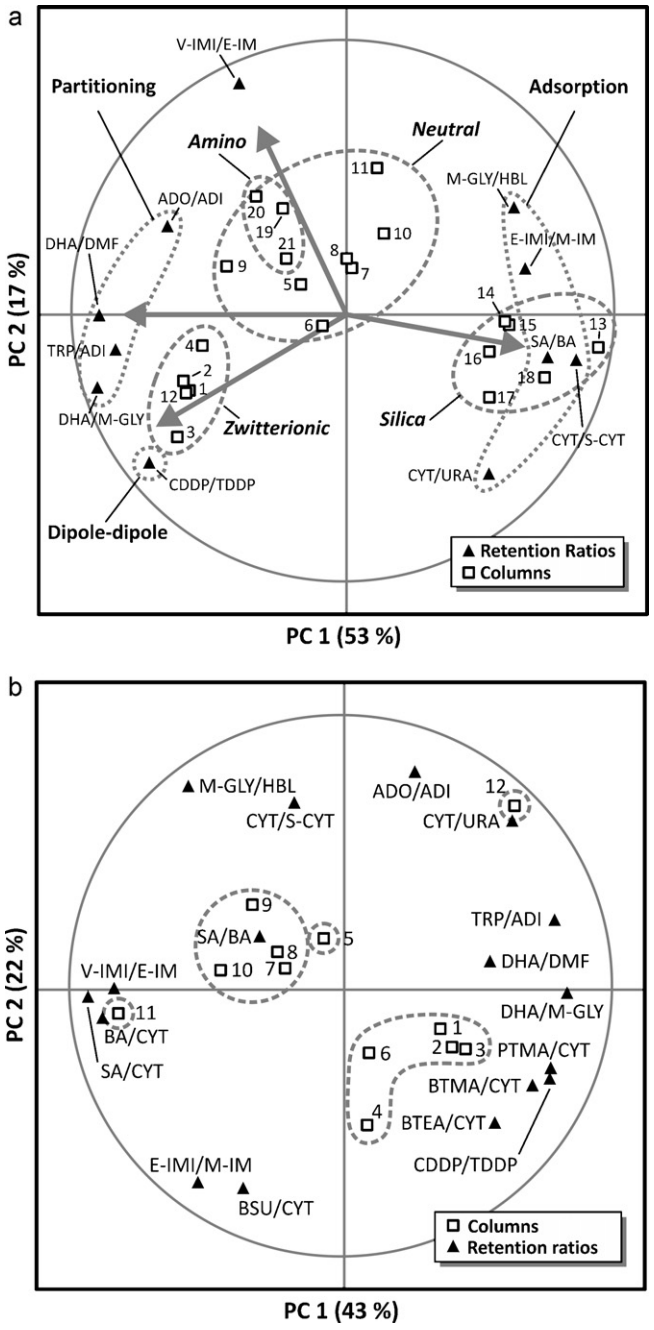

Fig. 6. Score and loading biplot of the two first component of the model where the observations were (a) all tested columns or (b) only neutral and zwitterionic columns, including PolySulfoethyl A, and the variables were the retention ratios of (a) all probe pairs except the anion and cation exchange probe pairs or (b) all probe pairs. For column numbering, see Table 2.

is also a prominent feature of the CYT/URA pair. Since CYT/S-CYT was not included in the design as a cation exchange probe, it was left in the model when all the dedicated anion and cation exchange pairs were masked, but its association with the silica columns could very well be due to the unintended dual function as an ion exchange probe, as elaborated above. The association of the plain silicas with the hydrophobic probe pair (E-IMI/M-IMI) and the hydrophobic shape selectivity probe pair (SA/BA), plus the fact that the Chromolith Si column, which showed the lowest retention of all tested columns (*cf.* Fig. 2) is the rightmost column in Figs. 4 and 5a are also highly interesting observations. We do not primarily interpret this as hydrophobic interactions being important for selectivity on the unmodified silicas, but rather as the silica columns having less hydrophilic selectivity than the other columns. It is also worth noting that Cogent Type C Silica (which is marketed as having some hydrophobic retention power) showed a selectivity pattern that clustered it with the other silica columns, both in the presence and absence of the ion exchange probe pairs. In other words, under the conditions of this test and with the probes selected, it was not possible to distinguish the HILIC retention pattern of the Type C silica from the other (Type A and B) silicas.

The amino columns remained well clustered together when the ion exchange probe pairs had been removed. However, the cluster had now moved substantially closer to the center of the plot and overlapped the rather diffuse cluster containing the neutral columns and the monomerically modified zwitterionic columns Shiseido PC HILIC and Nucleodur HILIC. An interesting observation is that the π–π interaction probe pair V-IMI/E-IMI was located alone in the same direction as the amino columns. However, as it was concluded above that this pair probably primarily acted as an inverse probe for cation exchange interaction selectivity, this is not interpreted as any interaction of the vinyl group of V-IMI with the lone pair electrons on the amino group.

Another way to study the polar retention mechanisms involved in HILIC without overshadowing by electrostatic interactions would be to eliminate all columns that were identified as being strongly correlated with ion exchange in Fig. 5. This would entail the amino and silica columns being masked out and a PCA being run on the remaining neutral and zwitterionic columns against all the probe pairs. This model also included PolySulfoethyl A, since this column had shown properties (Figs. 4 and 5a) that positioned it within the group of zwitterionic columns, notwithstanding being marketed as a cation exchange material. As expected, this maneuver of creating a model involving only the neutral/zwitterionic columns changed the appearance of the score-loading biplot quite radically, as seen in Fig. 6b.

All the zwitterionic columns, with the exception of Nucleodur HILIC, now grouped with the CDDP/TDDP, PTMA/CYT, BTMA/CYT, and BTEA/CYT probe pairs, and quite closely to the DHA/M-GLY, DHA/DMF and TRP/ADI probe pairs. In other words, all these columns showed a combination of dipole–dipole interaction, cation exchange properties, and multipoint (partitioning) interaction. Although electrostatic interactions attributable to cation exchange were evident, they were much weaker than for the underivatized silicas (Fig. 5). PolySulfoethyl A column was now clearly distinguished from Fig. 5 the neutral and zwitterionic columns, and was grouped with the probe pairs ADO/ADI and CYT/URA, which were designed to probe multipoint hydrogen bonding and general hydrophilic interactions. Thus, this model confirmed that cation exchange was not the most prominent interaction mode for the PolySulfoethyl A column, since it was located quite far away from the cation exchange probe pairs. The Nucleodur HILIC column was situated closer to the neutral columns than to the other zwitterionic columns. Although located in the same region of the plot, the polymer-based ZIC-pHILIC column showed somewhat different selectivity compared to the silica-based ZIC-HILIC columns, which all grouped very tightly together. Among the columns that were now located in the zwitterionic cluster, the Shiseido column with phosphocholine functionality was closer to the neutral columns. Together this strengthens the conclusion that zwitterionic columns with low ligand loading essentially behave as neutral, having limited contribution to selectivity from any ionic interactions and it furthermore indicates that the Nucleodur HILIC column would have lower zwitterionic density than any of the other zwitterionic columns. This conclusion would also imply that zwitterionic columns with high ligand density could expose measureable ionic interaction properties despite their presumed overall neutrality.

Somewhat surprising was to find the Luna HILIC, claimed to be based on a "crosslinked diol" functionality, closely associated with the anion exchange probes BA/CYT and SA/CYT and almost directly opposite to the multipoint hydrogen bonding probes ADO/ADI and the hydrophilic CYT/URA probes. If this would be due to ionic interactions, it would have been more rational to find traces of cation exchange properties in a silica-based column with intended neutral ligands. A more probable explanation for this clustering would thus be that the column had a negative correlation with the multipoint hydrogen bonding and hydrophilicity probes, meaning that selectivity for the Luna HILIC column mainly is derived from single point interactions and adsorption rather than partitioning. This is well in line with recent work on retention prediction models using molecular descriptors in HILIC separations on diol and poly(vinylalcohol)-based columns [45], where strong contributions from hydrogen bonding (particularly hydrogen donor) have been reported. Similarly, a significantly reduced tendency for diol columns to interact with ion exchange probes has been noted [32]. Still it cannot be ruled out that also the stationary phase support and/or unrevealed functionalities contributed to their HILIC retention mechanism to some extent.

3.7. Effect of pore diameter and particle size

The pore diameter of a separation material is inversely related to its specific surface area [46]. For example, the specific surface area of LiChrospher Si used in this work is 400 m^2/g for the 100 Å material and 700 m^2/g for the packing with 60 Å pore diameter. Pores of smaller diameter might also lead to more shape selective interactions. In Fig. 2 the effect of pore size is evident with the ZIC-HILIC (columns 2 and 3) and LiChrospher Silica (columns 16 and 17) where the retention times increased with decreasing pore diameter. As shown on the score plot unraveling selectivity (Fig. 5), the ZIC-HILIC columns with 100 and 200 Å pore size were less different from each other than they appear in Fig. 2, which only accounts for retention. This was also true for the 60 and 100 Å LiChrospher Silica columns. This again confirms that retention and selectivity are not necessarily related, and also shows that changes in pore diameter did not significantly change the selectivities of the HILIC materials for the low molecular weight probes used in this work.

Variations in the particle size should ideally affect neither the retention nor the selectivity of solutes on a set of columns with identical surface chemistry. Therefore, if a change in particle size affects the retention, other properties (specific surface area, density of surface functional group, etc.) of particles of different sizes must be different. In this work, the effects of particle size were studied on ZIC-HILIC with 3.5 and 5 μm particle size (columns 1 and 2) and TSKgel Amide 80 at 3 and 5 μm particle size (columns 7 and 8). As shown in Fig. 2, overall retentions for hydrophilic solutes on the two ZIC-HILIC columns were almost identical while those on the two TSKgel Amide 80 columns differed somewhat, with longer retention on the smaller particle size TSKgel Amide 80 column. The reason for this is unknown due to a lack of information about the composition and preparation of the materials. However, it was also noted that the difference in particle size did not change the selectivity of the TSKgel Amide 80 columns, since they were still located close to each other on the score plot (Fig. 5). This serves as validation of the model, which is intended to group columns based on selectivity.

3.8. Simplification of the model based on retention ratio

Since the ion-exchange solute pairs had been highly correlated in the earlier models (*cf.* Fig. 5), it was decided to keep only BTMA/CYT as cation exchange probe pair and BA/CYT as probe pair for anion exchange, to simplify the model for further studies. The

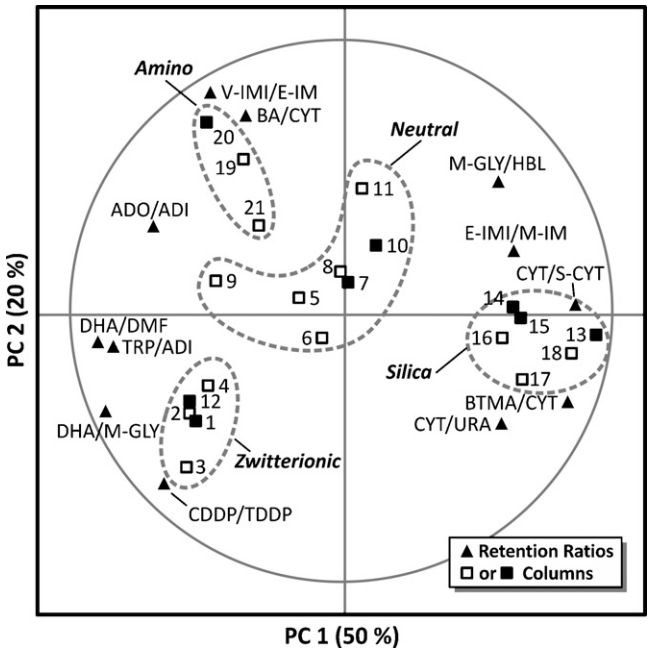

Fig. 7. Score and loading plot of simplified model based on separation factors of test substance pairs after elimination of all but one each of the anion and cation exchange markers. A filled column symbol denotes that this column was selected for the tests of electrolyte and water concentration, reported in Figs. 7 and 8. For column numbering, see Table 2.

SA/BA pair was further excluded due to a low contribution to the model (Fig. 5). The model resulting from this reduced probe pair set (Fig. 7) still gave a very similar classification of the HILIC columns, but using a substantial lower number of probes. The R2 and Q2 of the refined model with two first components were 0.706 and 0.441, respectively, which means the validity of the model was still acceptable.

3.9. Effect of electrolyte concentration on retention and selectivity of HILIC columns

In order to assess how variation in electrolyte concentration affected the different classes of HILIC columns, eight columns were selected from the complete column set, based on their scoring in the selectivity test (Fig. 5). These included ZIC-HILIC 5 μm, PolySulfoethyl A, TSKgel Amide 80 5 μm, LiChrospher Diol, Purospher NH_2, LiChrospher Si, Atlantis HILIC Si, and Chromolith Si, identified by filled symbols in Fig. 7. On these columns, all solutes were reinjected in an eluent composed of 80:20 (v/v) ACN/H_2O with ammonium acetate (pH ~ 6.8) at 20 mM instead of 5 mM total concentration. Fig. 8 shows the scores for the runs at 5 and 20 mM when the retention times were fitted to the simplified model shown in Fig. 7 (see Section 3.8 above).

The displacements of the apparent column characteristics as a result of increasing the electrolyte concentration were in different directions, but the general trend was that all columns with high scores moved towards the central (neutral) area of the plot. The interpretation must be that higher electrolyte concentration caused a decrease in the discrimination power between the columns (which means a decrease in selectivity) by reducing both ion exchange and multipoint hydrogen bonding interaction. The scores of the ZIC-HILIC and PolySulfoethyl A columns exhibited greater changes than did the other six columns. The cation exchange properties and multipoint interactions of these two columns appeared to be quite similar at 5 mM ammonium acetate, whereas the PolySulfoethyl A column exhibited a greater cation exchange, and

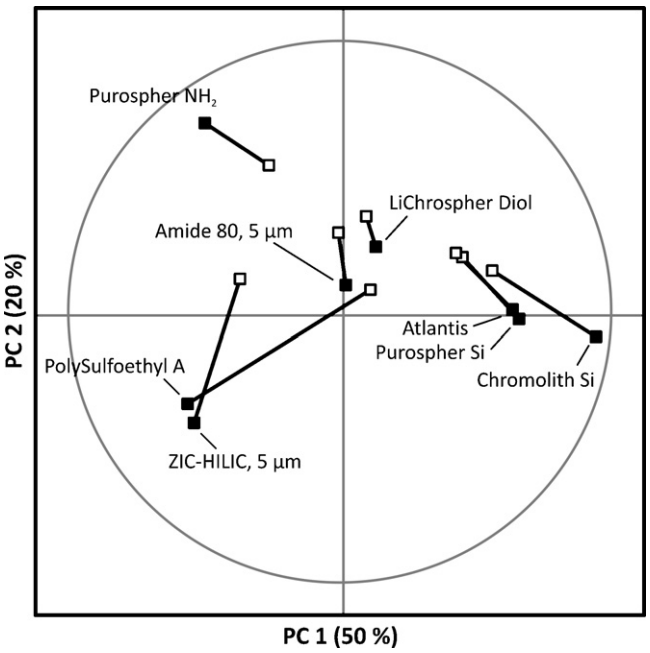

Fig. 8. Predicted score plot of columns run with the complete test solute set in eluents composed of ACN/H_2O 80:20 (v/v) with 5 mM (■) or 20 mM (□) ammonium acetate, pH ~ 6.8.

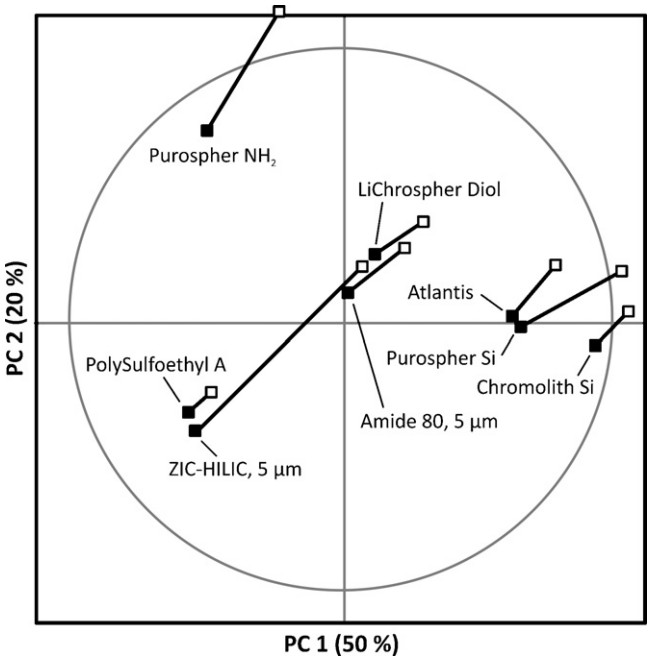

Fig. 9. Predicted score plot of columns run with the complete test solute set in eluents composed of 80:20 (■) or 70:30 (□) (v/v) ACN/H_2O containing 5 mM ammonium acetate, pH ~ 6.8.

significantly lower multipoint interaction than the ZIC-HILIC column at 20 mM ammonium acetate. This would again be consistent with shielding of residual opposite charges on the PolySulfoethyl A column. The reduced influence of ionic interactions at higher buffer salt concentrations have been noted previously and utilized to tune selectivity for charged species on zwitterionic columns [47]. The remaining strong influence of multipoint interactions on selectivity with the ZIC-HILIC column, could possibly be explained by a mechanism similar to the "anti-polyelectrolyte" or "salting-in" behavior that sulfobetaine type zwitterionic polymers show in aqueous solutions [48]. An increase in buffer salt concentration could thus lead to less self-association of the charges in the zwitterionic stationary phase, which potentially could result in a thicker and/or more hydrophilic layer for HILIC partitioning, provided that the stationary phase loading is sufficiently high.

3.10. Effect of eluent water content on retention and selectivity of HILIC columns

The same reduced column set used above was finally tested with an eluent consisting of ACN/H_2O 70:30 (v/v) and 5 mM ammonium acetate (pH ~ 6.8), and the retention times were then fitted to the simplified model, as above. The score plot with the eluents differing in water content is shown in Fig. 9. When the water content of the eluent was increased from 20 to 30%, all eight columns exhibited displacements in a direction involving less contribution from hydrogen bonding and dipole–dipole interactions. This unsurpringly verifies that hydrogen bonding and dipole–dipole interactions contribute significantly to the retention mechanism in HILIC. The ZIC-HILIC column was most affected by the increase in water content, and at 70:30 ACN/H_2O its selectivity pattern approached that of the neutral columns (LiChrosphere Diol and TSKgel Amide 80) chosen in the reduced column set. The PolySulfoethyl A column, which started out being very similar to the ZIC-HILIC column at 80:20 ACN/H_2O hardly changed its apparent selectivity on increasing the water content by 50%. It therefore appears as if the zwitterionic material responds more strongly than the other columns in the reduced test to changes in eluent water contents, and also required water concentrations below 30% to significantly express its characteristic selectivity.

4. Conclusions

Models based on the retention ratios of substance pairs showed better discrimination of columns than the retention factors of single substances, since selectivity and retention are not necessarily closely related in chromatography. The combination of test solutes in pairs plus principal component analysis has proven to be a valuable tool for characterizing HILIC columns with regards to interaction modes. Under the test conditions, the columns fell into four functional groups with respect to their main selectivity, as follows:

(i) Cation exchange – unmodified silicas;
(ii) Anion exchange – columns with amino functionality;
(iii) Dipole–dipole and multipoint hydrogen bonding – polymeric sulfobetaine, poly(2-sulfoethyl aspartamide);
(iv) Low specific interaction – hydroxyl, diol, amide, and monomeric zwitterionic.

A significant discrimination between HILIC columns could be made in terms of whether they rely mainly on adsorption and oriented hydrogen bonding for selectivity *vs.* if selectivity was established primarily *via* hydrophilic partitioning and multipoint interactions. All plain silica columns grouped close to adsorption selectivity, whereas zwitterionic columns generally showed a selectivity pattern that could be attributed to partitioning. In this respect, the neutral and amino columns occupied an intermediary position between the unmodified silicas and the zwitterionic columns.

This study also further confirmed that partitioning is the dominant mechanism in HILIC, with ion exchange being a powerful and orthogonal selectivity factor that can be used concurrently with the water content and combined with varying electrolyte concentrations to tailor-fit the retention for charged solutes. We failed to see any pronounced effects from π–π interaction. This

could either be due to such interactions being insignificant or to an unfortunate choice of probes. It should also be remarked that not only the intended functional groups but also "obscure" polar functionalities can contribute to the retention mechanism in HILIC. This was most obvious for PolySulfoethyl A which showed similarities to the zwitterionic columns in spite of its manifest strong cation exchange functionality, a peculiarity that might be ascribed either to the existence of residual amine groups or to condition-dependent cation-exchange behavior of the zwitterionic columns. The relationship between the selectivity and the HILIC column chemistry therefore still seems quite complicated, evident from columns claimed to possess a certain functional groups that in reality show a radically different selectivity. The true role of the functional group(s) was also an issue when probing the interaction mode.

Common for all material types tested was that reducing pore diameter led to longer retention, but did not significantly change the selectivities. The particle diameter was also demonstrated not to affect the selectivity of the columns significantly. Increased mobile phase water content primarily reduced the retention contributions attributable to hydrogen bonding and dipole–dipole interactions. These interactions therefore appear to play a major role in "hydrophilic interaction". Noteworthy from this study is also that an increasing electrolyte concentration led to a reduction in the disparities between column materials due to shielding of electrostatic interaction, both attractive and repulsive, as well as hydrogen bonding and dipole–dipole interactions. Thus, higher eluent salt concentrations led to a decrease in the unique selectivities of the different types of HILIC columns tested and made their retention patterns more similar. In other words, eluents with limited ionic strength should be employed to harvest the inherent selectivity potential in HILIC.

Acknowledgements

The authors thank Andrew Alpert for helpful discussions, and PolyLC Inc., Waters, and Tosoh Bioscience for supporting this work with columns. This work was financially supported by The Swedish Science Foundation (VR).

References

[1] P. Hemström, K. Irgum, J. Sep. Sci. 29 (2006) 1784.
[2] A.J. Alpert, J. Chromatogr. 499 (1990) 177.
[3] J.C. Linden, C.L. Lawhead, J. Chromatogr. 105 (1975) 125.
[4] J.K. Palmer, Anal. Lett. 8 (1975) 215.
[5] I.S. Krull, R.S. Strong, in: M. Cooke, C.F. Poole (Eds.), Encyclopedia of Separation Science, Academic Press, London, 2000, p. 583.
[6] S. Eksborg, P. Lagerström, R. Modin, G. Schill, J. Chromatogr. 83 (1973) 99.
[7] C.R. Mitchell, Y. Bao, N.J. Benz, S. Zhang, J. Chromatogr. B 877 (2009) 4133.
[8] K.J. Fountain, J. Xu, D.M. Diehl, D. Morrison, J. Sep. Sci. 33 (2010) 834.
[9] B. Dejaegher, Y.V. Heyden, J. Sep. Sci. 33 (2010) 698.
[10] M. Diener, K. Erler, B. Christian, B. Luckas, J. Sep. Sci. 30 (2007) 1821.
[11] A.J. Alpert, M. Shukla, A.K. Shukla, L.R. Zieske, S.W. Yuen, M.A.J. Ferguson, A. Mehlert, M. Pauly, R. Orlando, J. Chromatogr. A 676 (1994) 191.
[12] S.C. Churms, J. Chromatogr. A 720 (1996) 75.
[13] M. Wuhrer, A.R. de Boer, A.M. Deelder, Mass Spectrom. Rev. 28 (2009) 192.
[14] L.R. Ruhaak, C. Huhn, W. Waterreus, A.R. de Boer, C. Neusu, C.H. Hokke, A.M. Deelder, M. Wuhrer, Anal. Chem. 80 (2008) 6119.
[15] K. Spagou, H. Tsoukali, N. Raikos, H. Gika, I.D. Wilson, G. Theodoridis, J. Sep. Sci. 33 (2010) 716.
[16] Z. Hao, B. Xiao, N. Weng, J. Sep. Sci. 31 (2008) 1449.
[17] W. Naidong, J. Chromatogr. B 796 (2003) 209.
[18] J. Wu, W. Bicker, W. Lindner, J. Sep. Sci. 31 (2008) 1492.
[19] B.A. Olsen, J. Chromatogr. A 913 (2001) 113.
[20] Y. Guo, S. Gaiki, J. Chromatogr. A 1074 (2005) 71.
[21] J. Yu, Z. El Rassi, J. High Resolut. Chromatogr. 17 (1994) 773.
[22] J. Randon, S. Huguet, C. Demesmay, A. Berthod, J. Chromatogr. A 1217 (2010) 1496.
[23] T. Zhou, C.A. Lucy, J. Chromatogr. A 1187 (2008) 87.
[24] J. Randon, J.F. Guerrin, J.L. Rocca, J. Chromatogr. A 1214 (2008) 183.
[25] Z. Huang, M.A. Richards, Y. Zha, R. Francis, R. Lozano, J. Ruan, J. Pharm. Biomed. Anal. 50 (2009) 809.
[26] M. Guerrouache, A. Pantazaki, M.C. Millot, B. Carbonnier, J. Sep. Sci. 33 (2010) 787.
[27] E. Lesellier, C. West, J. Chromatogr. A 1158 (2007) 329.
[28] Y. Chen, W. Bicker, J. Wu, M.Y. Xie, W. Lindner, J. Chromatogr. A 1217 (2010) 1255.
[29] R.-I. Chirita, C. Westa, A.-L. Finaru, C. Elfakir, J. Chromatogr. A 1217 (2010) 3091.
[30] S. Van Dorpe, V. Vergote, A. Pezeshki, C. Burvenich, K. Peremans, B. De Spiegeleer, J. Sep. Sci. 33 (2010) 728.
[31] Y. Guo, S. Srinivasan, S. Gaiki, Chromatographia 66 (2007) 223.
[32] D.V. McCalley, J. Chromatogr. A 1217 (2010) 3408.
[33] B. Bard, P.-A. Carrupt, S. Martel, J. Med. Chem. 52 (2009) 3416.
[34] K. Kurdziel, T. Głowiak, Polyhedron 19 (2000) 2183.
[35] J.A. Joule, K. Mills, Heterocyclic Chemistry , 5th edition, Wiley, Hoboken, NJ, 2010, p. 461 ff.
[36] C.-X. Cao, Y.-Z. He, M. Li, Y.-T. Qian, M.-F. Gao, L.-H. Ge, S.-L. Zhou, L. Yang, Q.-S. Qu, Anal. Chem. 74 (2002) 4167.
[37] D.M. Jameson, G. Weber, J. Phys. Chem. 85 (1981) 953.
[38] M.M. Cardoso, M.J. Barradas, K.H. Kroner, J.G. Crespo, J. Chem. Technol. Biotechnol. 74 (1999) 801.
[39] D. Nolting, T. Schultz, I.V. Hertel, R. Weinkauf, Phys. Chem. Chem. Phys. 8 (2006) 5247.
[40] (a) http://www.shiseido.co.jp/e/hplc/column/html/ph_index.htm (accessed 08.12.10).;
(b) U.S. Pat. Appl. 2007/0241054 A1.
[41] http://www.mn-net.com/tabid/11114/default.aspx (accessed 08.12.10).
[42] A.J. Alpert, K. Petritis, L. Kangas, R.D. Smith, K. Mechtler, G. Mitulovic, S. Mohammed, A.J.R. Heck, Anal. Chem. 82 (2010) 5253.
[43] A.J. Alpert, P.C. Andrews, J. Chromatogr. 443 (1988) 85.
[44] M. Gilar, P. Olivova, A.E. Daly, J.C. Gebler, Anal. Chem. 77 (2005) 6426.
[45] K. Jinno, N.S. Quimming, N.L. Denola, Y. Saito, Anal. Bioanal. Chem. 393 (2009) 137–153.
[46] C.F. Poole, The Essence of Chromatography , Elsevier, Amsterdam, 2003, p. 271 ff.
[47] Y. Takegawa, K. Deguchi, H. Ito, T. Keira, H. Nakagawa, S.-I. Nishimura, J. Sep. Sci. 29 (2006) 2533–2540.
[48] C. Konak, R.C. Rathi, P. Kopecek, Macromolecules 27 (1994) 1992–1996.
[49] http://ntp.niehs.nih.gov/index.cfm?objectid=E87E09E6-BDB5-82F8-F72267F0C9323EA1 (accessed 08.11.10).
[50] http://www.chemaxon.com/products/calculator-plugins (accessed 08.12.10).